Numerical Simulation of the Dispersion of Pollutant in a Canal

Abstract

In this work, we propose a numerical approach to model 2D pollutant dispersion in a canal using the famous advection-reaction diffusion equations. The advection-dispersion equation model describes transport and diffusion problems as seen in the mixing of conservative, nonbuoyant pollutants deposited into a stream or canal. The canal consisted of a narrow channel that allows inflow of water through an entry opening, and outflow through an exit opening. We obtain stability conditions for finite difference schemes and show the existence and uniqueness of solutions for the finite element method. The simulations show that the concentration of pollutants in the canal is controlled by the divergence term and increases in the direction of fluid flow.

1. Introduction

The adverse effects of pollution on man and the environment have been noticeable for centuries but have assumed significant heights in recent years due to the industrial revolution. Pollutions such as air pollution and water pollution pose serious threats to both plants and animals, including humans. Thus, the possibility of measuring the concentration of pollutants and understanding the dynamics of dispersion in the particular medium of concern would make it possible to check on the adverse effects. Carrying out such analytical tasks may be physically tedious and may not capture the details and critical aspects of the process. Hence, the importance of mathematical models in proffering solutions to real-life problems. A mathematical model comprises of independent and dependent variables and a system of relationships in the form of equation or inequality that exist between the variables. The problem is modelled by a governing mathematical equation that considers the important aspects of the problem. Then where analytical solutions are intractable, numerical methods are adopted to solve the equation.

In [1], mathematical modelling of pollutant dispersion in natural streams is proposed. The dispersion is considered longitudinal and one-dimensional in the flow direction. The Transmission Line Matrix (TLM), which provides a significant gain in computing time, is used for numerical computations. In [2], the dispersion 1D longitudinal flow has been studied extensively. In [3], the authors proposed calibrating pollutant dispersion in 1D hydraulic models of river networks utilizing a central difference scheme. The river networks were modelled utilizing Mage.

In [4], a numerical technique has been employed to study and analyze water quality in a reservoir. 2D models have been used to model the reservoir's pollutant concentration. The hydrodynamic model and the dispersion model used the Lax-Wendroff method for water flow and its elevation. A forward difference scheme in time and a spatial central scheme were to simulate pollutant concentration. In [5], mathematical modelling of water pollutant control in a connected reservoir system is proposed using an implicit finite difference scheme. The reservoir system was in the form of two ponds connected by a tunnel. Two mathematical models were employed in the simulation. The first model was a static dispersion model which modelled the pollutant level in the reservoir system. The second model controlled the pollution levels within the ponds. In [6], the researchers developed two techniques for measuring salinity intrusion in a stream. The first method used the forward time centred space scheme, while the second adopted the MacCormack scheme with function interpolation at the boundary points. A comparison of the result with the exact solution indicated that the MacCormack scheme is more efficient. In [7], the authors modelled the space-time effect of water pollution resulting from industrial wastes. They employed a two-dimensional numerical algorithm to solve the equations of mass concentration, momentum, and chemical concentration inflow. The output indicated that pollutants flowed downstream, causing more areas to be polluted but with less concentration. This has a devastating effect on the aquatic life in the water, and water usability. In [8], the researchers employed numerical simulations and in-situ sampling to investigate the space-time changes of non-point source pollution in a small urban locality. The simulations identified residential, industrial, and commercial lands as main sources of pollutant loading, and as pollution prone areas.

In this study, pollutants behaviour in a canal is observed through numerical simulations of a two-dimensional advection-dispersion equation. The numerical solutions of the equation were obtained using both explicit and implicit difference schemes, and the finite element method. Firstly, the finite difference method was implemented. We discretized the model equation using the theta scheme and obtained the stability conditions for the finite difference schemes. Simulations of pollutant dispersion were carried out with and without inclusion of the divergence term. Secondly, we consider a rectangular domain. The solution of the model equation and the boundary conditions is obtained with the aid of the FreeFem++ software [9]. We compute the approximate solution by a finite element method of Lagrange type P1 for the spatial discretization. An Euler method is used for the time discretization. The interest of this method is the possibility of considering unstructured geometries.

2. Two-Dimensional Model

2.1. The Governing Equation

In this section, we consider the parabolic equation. The mathematical model describing the transport and dispersion processes is a two-dimensional advection-dispersion equation (ADE).

$$\frac{\partial \rho}{\partial t} - v\Delta\rho + div(\vec{v}\rho) = f(x,y,t), \quad \forall (x,y) \in \Omega, t > 0 \qquad (1)$$

2.2. Initial and Boundary conditions

The initial conditions are

$$\rho(x,y,0) = 0 \quad \forall(x,y)\epsilon\Omega$$

$$\rho(x,y,t) = 0 \quad \forall(x,y)\epsilon\Gamma_2$$

And the boundary conditions are

$$\frac{\partial \rho}{\partial t} = 0, \forall(x,y)\epsilon\Gamma_1, t > 0$$

$$\frac{\partial \rho}{\partial \vec{n}} = g(x,y,t), \forall(x,y)\epsilon\Gamma_3, t > 0$$

Where $\rho(x,y,t)$ is the function that gives the concentration of a pollutant at each point (x,y) at time t. We consider a bounded media $\Omega \subset \mathbb{R}^2$, with the border $\partial\Omega$ divided into three parts: Γ_1 the walls, Γ_2 the entering boundary of the non-polluted fluid and Γ_3 the outer boundary. The velocity of the fluid is given by the vector function $v(x,y,t)$, which is tangential to the horizontal walls:

$$\vec{v}(x,y,t) \cdot \vec{n}(x,y) = 0 \, \forall(x,y)\epsilon\Gamma_1, \forall t > 0$$

Where $\vec{n}(x,y)$ is the outward normal to Ω at the point (x,y). v is the dispersion constant and a function $g(x,y,t)$ defined in $\Gamma_3 \times \mathbb{R}^+$ models the outward flux of pollutant. Moreover, the function $f(x,y,t)$ acts as a source term and models the injection of the pollutant in the canal.

We will limit to the following special case:

$\Omega =]0, L[\times]0, h[, \, \vec{v}(x,y,t) = (1,0)$ and $g(x,y,t) = c,$

Where c is a constant. We will always take right-hand side f with limited support in space (example a Dirac), and we make simulations with the following possible values:

$$f(x,y,t) = \delta_{x0}\delta_{y0} \quad or$$

$$f(x,y,t) = \delta_{x0}\delta_{y0} * t * (1-t) * \chi_{[0,1]}$$

3. Numerical Technique

3.1. Finite Difference Implementation Using θ-Scheme

The equation (1) is approximated by a finite difference method in space and the θ-scheme for the time discretization. Then the values contours of the solution are traced for different right-hand side f. Furthermore, the solutions are compared for different values of θ.

The solution domain of the problem is covered by a mesh of grid lines [10]. The grid point (x_i, y_j, t) is defined by $x_i = i\Delta x$, $y_j = j\Delta y$ for all $i = 0,1,2,\ldots, M_x$, and $j = 0,1,2,\ldots, M_y$.

The θ-scheme is given by

$$\frac{\partial \rho}{\partial t} = F(\rho)$$

$$\frac{\rho^{n+1} - \rho^n}{\Delta t} = F\big((1-\theta)\rho^{n+1} + \theta\rho^n\big)$$

$$= \frac{d}{dt}\big((1-\theta)\rho^{n+1} + \theta\rho^n\big)$$

$$= (1-\theta)\frac{d}{dt}\rho^{n+1} + \theta\frac{d}{dt}\rho^n$$

$$= (1-\theta)F(\rho^{n+1}) + \theta F(\rho^n)$$

Given that $\vec{v}(x,y,t) = (1,0)$, and taking g as a constant, the problem in equation (1) becomes $\frac{\partial \rho}{\partial t} = v\Delta\rho + \frac{\partial \rho}{\partial x} = f$

Discretizing the above equation we obtain:

$$\frac{\rho_{i,j}^{n+1}-\rho_{i,j}^n}{\Delta t} - v\left(\frac{\rho_{i+1,j}^{n+1}-2\rho_{i,j}^{n+1}+\rho_{i-1,j}^{n+1}}{\Delta x^2} + \frac{\rho_{i,j+1}^{n+1}-2\rho_{i,j+1}^{n+1}+\rho_{i,j-1}^{n+1}}{\Delta y^2}\right)(1-\theta) + \left(\frac{\rho_{i,j}^{n+1}-\rho_{i-1,j}^{n+1}}{\Delta x}\right)(1-\theta) - v\theta\left(\frac{\rho_{i+1,j}^n-2\rho_{i,j}^n+\rho_{i-1,j}^n}{\Delta x^2}\right) +$$

ρi,j+1n−2ρi,j+1n+ρi,j−1nΔy2 +θρi,jn−ρi−1,jnΔx=1−θFi,jn+1+θFi,jn

Simplifying further and taking the value of $\theta = 1$ the Euler Explicit method, and we have our discretization as follow;

$$\frac{\rho_{i,j}^{n+1} - \rho_{i,j}^n}{\Delta t} - v\left(\frac{\rho_{i+1,j}^{n+1} - 2\rho_{i,j}^{n+1} + \rho_{i-1,j}^{n+1}}{\Delta x^2} + \frac{\rho_{i,j+1}^{n+1} - 2\rho_{i,j+1}^{n+1} + \rho_{i,j-1}^{n+1}}{\Delta y^2}\right) + \frac{\rho_{i,j}^n - \rho_{i-1,j}^n}{\Delta x} = f$$

Analyzing the stability using the Fourier function

$$f(u)(\epsilon,\eta) = \hat{u}(\epsilon,\eta) = \frac{1}{2}\pi \sum_{i,j=-\infty}^{\infty} e^{-ki\epsilon-kj\eta}\,\hat{u}_{i,j}$$

where k denotes the complex part. Let $r_x = \Delta t/\Delta x^2$ and $r_y = v\Delta t/\Delta y^2$. Now, substituting all these in equation (13) and setting $v = 1$ we have

$$\hat{u}^{n+1}(\epsilon,\eta) = \hat{u}^n(\epsilon,\eta) + r_x(e^{-k\epsilon}\hat{u}^n(\epsilon,\eta) - 2\hat{u}^n(\epsilon,\eta) + e^{k\epsilon}\hat{u}^n(\epsilon,\eta) - \hat{u}^n(\epsilon,\eta)\Delta x + e^{k\epsilon}\hat{u}^n(\epsilon,\eta)\Delta x)$$

$$+ r_y\left(e^{-k\eta}\hat{u}^n(\epsilon,\eta) - 2\hat{u}^n(\epsilon,\eta) + e^{-k\eta}\hat{u}^n(\epsilon,\eta)\right)$$

$$= [1 + r_x\left(e^{-k\epsilon} - (\Delta x + 2) + e^{k\epsilon}(\Delta x + 1)\right) + r_y(e^{-k\eta} - 2 + e^{k\eta})]\hat{u}^n(\epsilon,\eta)$$

Then we have

$$\hat{u}^{n+1}(\epsilon,\eta) = p(\epsilon,\eta)\hat{u}^n(\epsilon,\eta)$$

where p is referred to as the symbol of the difference scheme, it is the multiplier between the step n and step $n + 1$.

$$p = 1 + r_x\left(e^{-k\epsilon} - (\Delta x + 2) + e^{k\epsilon}(\Delta x + 1)\right) + r_y(e^{-k\eta} - 2 + e^{k\eta})$$

$$= 1 + r_x(2\cos\epsilon - (\Delta x + 2) + \Delta xe^{k\epsilon}) + 2r_y(\cos\eta - 1)$$

$$= 1 + r_x(-4\sin^2 c/2 + \Delta x(e^{k\epsilon} - 1) - 4r_y\sin^2 c/2)$$

Applying $\hat{u}^{n+1}(\epsilon,\eta) = p(\epsilon,\eta)\hat{u}^n(\epsilon,\eta)$, $n + 1$ times yields $\hat{u}^{n+1} = p^{n+1}\hat{u}^0$

Then we have $|\hat{u}^{n+1}| \leq |\hat{u}^0| \Longrightarrow |p| \leq 1$

Thus the condition for stability is

$$\Delta t \leq \frac{1}{2}\left(\frac{\Delta x^2\Delta y^2}{\Delta y^2 + \Delta x^2}\right)$$

Thus, for a given value of Δx and Δy, the allowed value of Δt must be such that it satisfies equation 14. Also, if $\Delta x = \Delta y$ we have,

$$\Delta t \leq \frac{1}{4}\Delta x^2$$

.

Taking the time and the divergence term is zero, we have a reduced scheme as

$$\left(\frac{2v}{\Delta x^2} + \frac{2v}{\Delta y^2}\right)\rho_{i,j} = v\left(\frac{\rho_{i+1,j} + \rho_{i-1,j}}{\Delta x^2} + \frac{\rho_{i,j+1} + \rho_{i,j-1}}{\Delta y^2}\right) + f$$

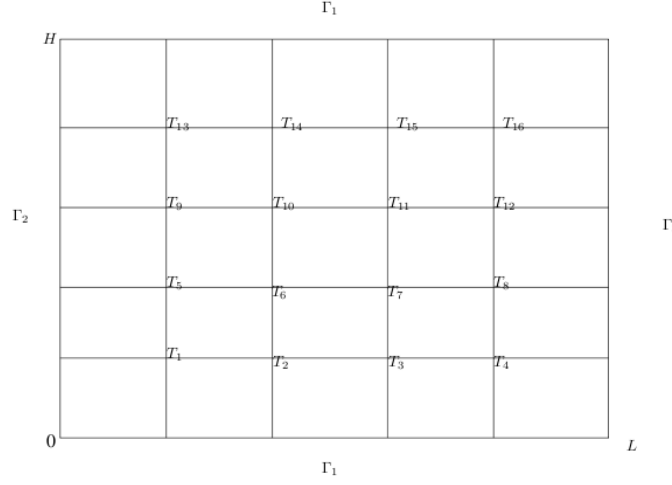We have the finite difference mesh as follows;

Figure 1: finite-difference mesh for the pollutant problem

3.2. Iterative Method for Boundary Value Problem

Applying the boundary conditions in order to write out the algorithm to solve this problem, we have the following set of equations;

For $i = 1$, $j = 1$,

$$\rho_{1,1} = \left(\frac{\Delta x^2 \Delta y^2}{2v\Delta y^2 + v\Delta x^2}\right)\left[v\left(\frac{\rho_{2,1}}{\Delta x^2} + \frac{\rho_{1,2}}{\Delta y^2}\right) + f\right]$$

For $i = 1$, $j = 2: M_y = 1$,

$$\rho_{1,j} = \left(\frac{\Delta x^2 \Delta y^2}{2v\Delta y^2 + 2v\Delta x^2}\right)\left[v\left(\frac{\rho_{2,j}}{\Delta x^2} + \frac{\rho_{1,j+1} + \rho_{1,j-1}}{\Delta y^2}\right) + f\right]$$

For $i = 1$, $j = M_y$,

$$\rho_{1,M_y} = \left(\frac{\Delta x^2 \Delta y^2}{2v\Delta y^2 + 2v\Delta x^2}\right)\left[v\left(\frac{\rho_{2,M_y}}{\Delta x^2} + \frac{\rho_{1,M_y+1} + \rho_{1,M_y-1}}{\Delta y^2}\right) + f\right]$$

For $i = 2: M_x = 1$, $j = 1$,

$$\rho_{i,1} = \left(\frac{\Delta x^2 \Delta y^2}{2v\Delta y^2 + v\Delta x^2}\right)\left[v\left(\frac{\rho_{i+1,1} + \rho_{i-1,1}}{\Delta x^2} + \frac{\rho_{i,2}}{\Delta y^2}\right) + f\right]$$

For $i = M_x$, $j = 1$,

$$\rho_{M_x,1} = \left(\frac{\Delta x^2 \Delta y^2}{2v\Delta y^2 + v\Delta x^2}\right)\left[v\left(\frac{\rho_{M_x-1,1}}{\Delta x^2} + \frac{\rho_{M_x,2}}{\Delta y^2}\right) + \frac{vg}{\Delta x} + f\right]$$

For $i = M_x$, $j = 2, M_y = 1$,

$$\rho_{M_x,j} = \left(\frac{\Delta x^2 \Delta y^2}{v\Delta y^2 + 2v\Delta x^2}\right)\left[v\left(\frac{\rho_{M_x-1,j}}{\Delta x^2} + \frac{\rho_{M_x,j+1} + \rho_{M_x,j-1}}{\Delta y^2}\right) + \frac{vg}{\Delta x} + f\right]$$

For $i = M_x$, $j = M_y$,

$$\rho_{M_x,M_y} = \left(\frac{\Delta x^2 \Delta y^2}{v\Delta y^2 + v\Delta x^2}\right)\left[v\left(\frac{\rho_{M_x-1,M_y}}{\Delta x^2} + \frac{\rho_{M_x,M_y-1}}{\Delta y^2}\right) + \frac{vg}{\Delta x} + f\right]$$
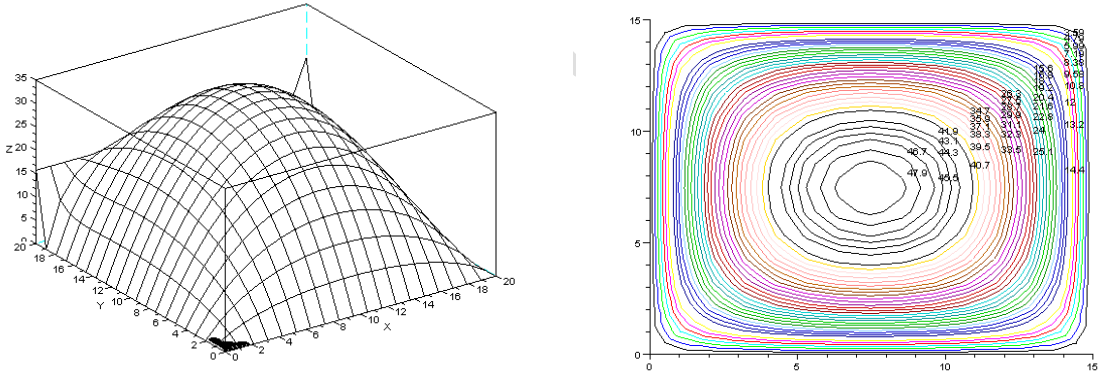
For $i = 2: M_x = 1$, $j = M_y$,

$$\rho_{i,M_y} = \left(\frac{\Delta x^2 \Delta y^2}{2v\Delta y^2 + v\Delta x^2}\right)\left[v\left(\frac{\rho_{i+1,M_y} + \rho_{i-1,M_y}}{\Delta x^2} + \frac{\rho_{i,M_y-1}}{\Delta y^2}\right) + \frac{vg}{\Delta x} + f\right]$$

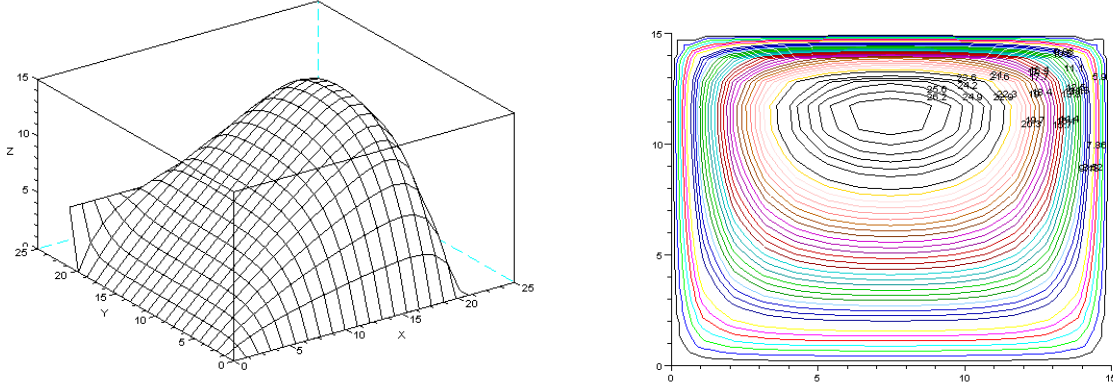For $i = 2: M_x = 1$, $j = 2, M_y = 1$,

$$\rho_{i,j} = \left(\frac{\Delta x^2 \Delta y^2}{2v\Delta y^2 + v\Delta x^2}\right)\left[v\left(\frac{\rho_{i+1,j} + \rho_{i-1,j}}{\Delta x^2} + \frac{\rho_{i,j+1} + \rho_{i,j-1}}{\Delta y^2}\right) + \frac{vg}{\Delta x} + f\right]$$

Implementing the above algorithm in Scilab we have the following:

(a) solution of the Poisson problem (b) contour for the Poisson problem
Figure 2: solution of the Poisson problem with $g = 0.08, a = 1, f = 3$

(a) solution of the problem with the divergence term (b) contour of the problem with divergence term

Figure 3: Solution the problem with $g = 0.08, a = 1, f = 3$

Figure 2 shows the solution to the Poisson part of the problem. It is observed that the concentration of the pollutant is higher inside the canal. Figure 3 shows the solution when the divergence term is included. The concentration of the pollutant is higher in the x-direction because the divergence term acts in this direction.

3.2.1. Explicit Euler Method

Now we consider the entire equation which is the explicit Euler scheme, we have the scheme as:

$$\frac{\rho_{i,j}^{n+1} - \rho_{i,j}^n}{\Delta t} - v\left(\frac{\rho_{i+1,j}^n - 2\rho_{i,j}^n + \rho_{i-1,j}^n}{\Delta x^2} + \frac{\rho_{i,j+1}^n - 2\rho_{i,j+1}^n + \rho_{i,j-1}^n}{\Delta y^2}\right) + \frac{\rho_{i,j}^n - \rho_{i-1,j}^n}{\Delta x} = f$$

The equation above can be written as

$$\rho_{i,j}^{n+1} = \rho_{i,j}^n + \Delta t v\left(\frac{\rho_{i+1,j}^n - 2\rho_{i,j}^n + \rho_{i-1,j}^n}{\Delta x^2} + \frac{\rho_{i,j+1}^n - 2\rho_{i,j+1}^n + \rho_{i,j-1}^n}{\Delta y^2}\right) + \Delta t\frac{(\rho_{i,j}^n - \rho_{i-1,j}^n)}{\Delta x} + \Delta t f$$

For $i = 1, j = 1$,

$$\rho_{1,1}^{n+1} = \rho_{1,1}^n + \Delta t v\left(\frac{\rho_{2,1}^n - 2\rho_{1,1}^n}{\Delta x^2} + \frac{\rho_{1,2}^n - \rho_{1,1}^n}{\Delta y^2}\right) + \frac{\Delta t}{\Delta x}\rho_{1,1}^n + \Delta t f$$

For $i = 1, j = 2: M_y = 1$,

$$\rho_{1,1}^{n+1} = \rho_{1,1}^n + \Delta t v\left(\frac{\rho_{2,j}^n - 2\rho_{1,j}^n}{\Delta x^2} + \frac{\rho_{1,2}^n - 2\rho_{1,j}^n + \rho_{1,j-1}^n}{\Delta y^2}\right) + \frac{\Delta t}{\Delta x}\rho_{1,j}^n + \Delta t f$$

For $i = 1, j = M_y$,

$$\rho_{1,M_y}^{n+1} = \rho_{1,M_y}^n + \Delta t\nu\left(\frac{\rho_{2,M_y}^n - 2\rho_{1,M_y}^n}{\Delta x^2} + \frac{\rho_{1,M_y-1}^n - \rho_{1,M_y}^n}{\Delta y^2}\right) + \frac{\Delta t}{\Delta x}\rho_{1,M_y}^n + \Delta tf$$

For $i = 2: M_x = 1, j = 1$,

$$\rho_{i,1}^{n+1} = \rho_{i,1}^n + \Delta t\nu\left(\frac{\rho_{i+1,1}^n - 2\rho_{i,1}^n + \rho_{i-1,1}^n}{\Delta x^2} + \frac{\rho_{i,2}^n - \rho_{i,1}^n}{\Delta y^2}\right) + \Delta t\frac{(\rho_{i,1}^n - \rho_{i-1,1}^n)}{\Delta x} + \Delta tf$$

For $i = M_x, j = 1$,

$$\rho_{M_x,1}^{n+1} = \rho_{M_x,1}^n + \Delta t\nu\left(\frac{\rho_{M_x+1,1}^n - \rho_{M_x,1}^n}{\Delta x^2} + \frac{\rho_{M_x,2}^n - \rho_{M_x,1}^n}{\Delta y^2}\right) + \Delta t\frac{(\rho_{M_x,1}^n - \rho_{M_x-1,1}^n - vg)}{\Delta x} + \Delta tf$$

For $i = M_x, j = 2, M_y = 1$,

$$\rho_{M_x,j}^{n+1} = \rho_{M_x,j}^n + \Delta t\nu\left(\frac{\rho_{M_x-1,j}^n - \rho_{M_x,j}^n}{\Delta x^2} + \frac{\rho_{M_x,j+1}^n - 2\rho_{M_x,j}^n + \rho_{M_x-1,j-1}^n}{\Delta y^2}\right) - \Delta t\frac{(\rho_{M_x,j}^n - \rho_{M_x-1,j}^n - vg)}{\Delta x} + \Delta tf$$
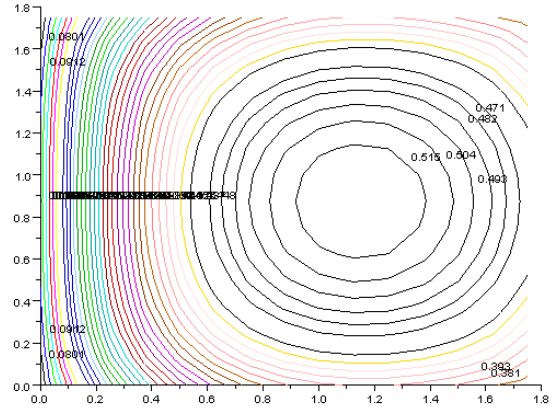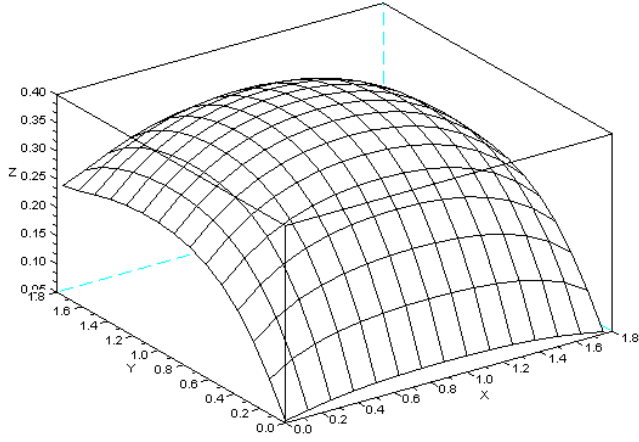
For $i = M_x, j = M_y$,

$$\rho_{M_x,M_y}^{n+1} = \rho_{M_x,M_y}^n + \Delta t\nu\left(\frac{\rho_{M_x-1,M_y}^n - \rho_{M_x,M_y}^n}{\Delta x^2} + \frac{\rho_{M_x,M_y-1}^n - \rho_{M_x,M_y}^n}{\Delta y^2}\right) - \Delta t\frac{(\rho_{M_x,M_y}^n - \rho_{M_x-1,M_y}^n - vg)}{\Delta x} + \Delta tf$$

For $i = 2: M_x - 1, j = M_y$,

$$\rho_{i,M_y}^{n+1} = \rho_{i,M_y}^n + \Delta t\nu\left(\frac{\rho_{i+1,M_y}^n - 2\rho_{i,M_y}^n + \rho_{i-1,M_y}^n}{\Delta x^2} + \frac{\rho_{i,M_y-1}^n - \rho_{i,M_y-1}^n}{\Delta y^2}\right) - \Delta t\frac{(\rho_{i,M_y}^n - \rho_{i-1,M_y}^n)}{\Delta x} + \Delta tf$$

For $i = 2: M_x - 1, j = 2: M_y - 1$,

$$\rho_{i,j}^{n+1} = \rho_{i,j}^n + \Delta t\nu\left(\frac{\rho_{i+1,j}^n - 2\rho_{i,j}^n + \rho_{i-1,j}^n}{\Delta x^2} + \frac{\rho_{i,j-1}^n - 2\rho_{i,j}^n + \rho_{i,j}^n}{\Delta y^2}\right) - \Delta t\frac{(\rho_{i,j}^n - \rho_{i-1,j}^n)}{\Delta x} + \Delta tf$$

a) solution of the problem for explicit Euler (b) contour of the problem for explicit Euler

Figure 4: Solution to the pollutant problem for explicit Euler with $g = 0.08, a = 1, f = 3$

It is noted from Figure 4 above that as the source term increases, the pollutant increases and as such, there is more concentration inside the canal. The pollutant increases with time until it reaches a maximum threshold after which it remains constant.

3.2.2. Implicit Euler Method

Taking $\theta = 0$ we have the implicit Euler. We have the discretized scheme as

$$\frac{1}{\Delta y^2}\rho_{i,j+1}^{n+1} - \frac{v}{\Delta x^2}\rho_{i+1,j+1}^{n+1} + \left(\frac{1}{\Delta t} + \frac{2v}{\Delta x^2} + \frac{2v}{\Delta y^2} + \frac{1}{\Delta x}\right)\rho_{i,j}^{n+1} + \frac{1}{\Delta y^2}\rho_{i,j}^{n+1} - \left(\frac{2v}{\Delta x^2} + \frac{1}{\Delta x}\right)\rho_{i-1,j}^{n+1} = f + \frac{\rho_{i,j}^n}{\Delta t}$$

From the above scheme, we have a system as

$$Au^{n+1} = \frac{1}{\Delta t}u^n + b, b = f + bc$$

where f is the right-hand side of the equation and bc is a contribution from the boundary condition, A is the non-symmetric matrix which is of the form. For example for a 3×3 matrix we have a matrix of the form:

$$A = \begin{bmatrix} a & -v/dx^2 & 0 & -v/dy^2 & 0 & 0 & 0 & 0 & 0 \\ b & a & -v/dx^2 & 0 & -v/dy^2 & 0 & 0 & 0 & 0 \\ 0 & b & c & 0 & 0 & -v/dy^2 & 0 & 0 & 0 \\ -v/dy^2 & 0 & 0 & f & -v/dx^2 & 0 & -v/dy^2 & 0 & 0 \\ 0 & -v/dy^2 & 0 & b & f & -v/dx^2 & 0 & -v/dy^2 & 0 \\ 0 & 0 & -v/dy^2 & 0 & b & c & 0 & 0 & -v/dy^2 \\ 0 & 0 & 0 & -v/dy^2 & 0 & 0 & a & -v/dx^2 & 0 \\ 0 & 0 & 0 & 0 & -v/dy^2 & 0 & b & a & -v/dx^2 \\ 0 & 0 & 0 & 0 & 0 & -v/dy^2 & 0 & b & c \end{bmatrix}$$

Where,

$$a = \frac{1}{\Delta t} + \frac{2v}{\Delta x^2} + \frac{v}{\Delta y^2} + \frac{1}{\Delta x},$$
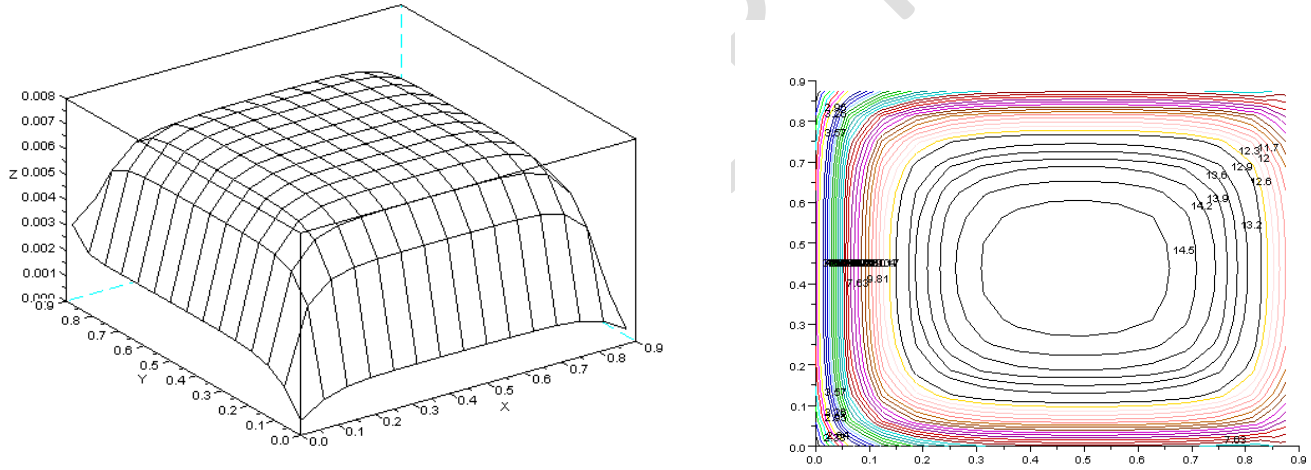
$$b = -\left(\frac{2v}{\Delta x^2} + \frac{1}{\Delta x}\right),$$

$$c = \frac{1}{\Delta t} + \frac{v}{\Delta x^2} + \frac{v}{\Delta y^2} + \frac{1}{\Delta x},$$

$$e = \frac{1}{\Delta t} + \frac{v}{\Delta x^2} + \frac{2v}{\Delta y^2} + \frac{1}{\Delta x},$$

$$f = \frac{1}{\Delta t} + \frac{2v}{\Delta x^2} + \frac{2v}{\Delta y^2} + \frac{1}{\Delta x}$$

Applying the Gauss Seidel method within the time loop, the convergence rate was found to be faster. The solution for the Implicit Euler is as follows:

a) solution of the problem for implicit Euler (b) contour of the problem for Implicit Euler
Figure 5: Solution to the pollutant problem implicit scheme with $g = 0.08, a = 1, f = 3$

From Figure 5, it is noted that the implicit Euler scheme gives a better solution than the explicit Euler scheme.
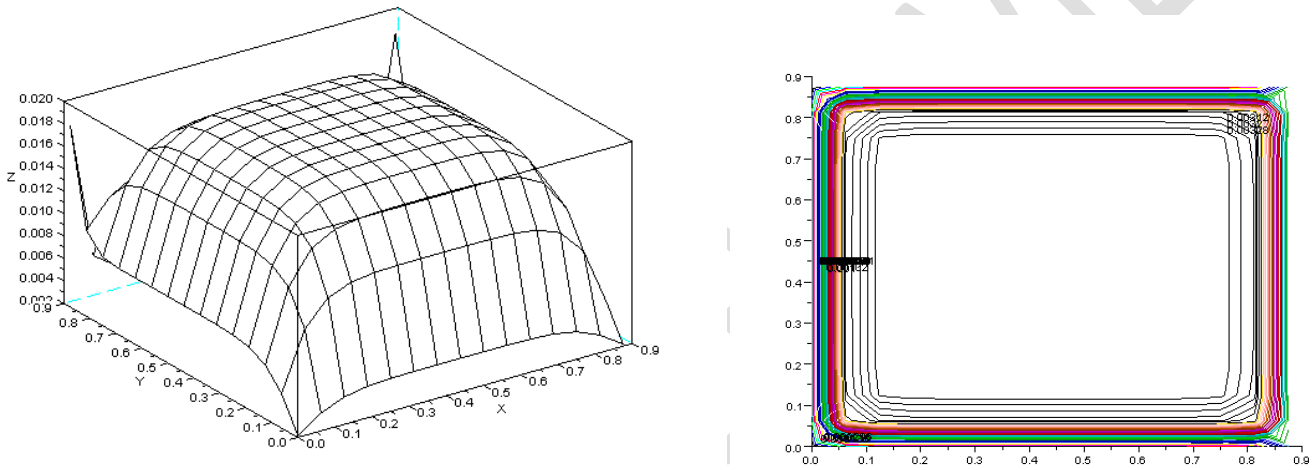
3.2.3. Crank Nicolson scheme

Taking $\theta = 1/2$ the Crank Nicolson scheme is obtained. The discretized scheme is

$$\left(\frac{1}{\Delta t} + \frac{v}{\Delta x^2} + \frac{v}{\Delta y^2} + \frac{1}{2}\frac{1}{\Delta x}\right)\rho_{i,j}^{n+1} - \frac{1}{2}\frac{1}{\Delta x^2}\rho_{i+1,j}^{n+1} - \frac{1}{2}\left(\frac{v}{\Delta x^2} + \frac{1}{\Delta x}\right)\rho_{i-1,j}^{n+1} - \frac{1}{2}\frac{v}{\Delta y^2}\rho_{i,j+1}^{n+1} - \frac{1}{2}\frac{v}{\Delta x^2}\rho_{i,j-1}^{n+1}$$

$$= \frac{1}{2}\left(\frac{v}{\Delta x^2} + \frac{1}{\Delta x}\right)\rho_{i-1,j}^n + \frac{1}{2}\frac{v}{\Delta x^2}\rho_{i+1,j}^n + \left(\frac{1}{\Delta t} + \frac{v}{\Delta x^2} + \frac{v}{\Delta y^2} + \frac{1}{2}\frac{1}{\Delta x}\right)\rho_{i,j}^{n+1} + \frac{1}{2}\frac{1}{\Delta y^2}\rho_{i,j+1}^{n+1}$$

$$+ \frac{1}{2}\frac{1}{\Delta y^2}\rho_{i,j-1}^{n+1}$$

From the above discretized scheme, we get a system as

$$Au^{n+1} = Bu^n + b, \qquad b = f + bc$$

Using Scilab we have the solution for the Crank Nicolson as follow:

(a) solution of the problem for Crank Nicolson (b) contour of the problem for Crank Nicolson
Figure 6: Solution to the pollutant problem Crank Nicolson scheme with $g = 0.08, a = 1, f = 3$

In Figure 6, the Crank Nicolson scheme (an improved implicit Euler scheme) also gives a better result. It is noted that the pollutant reaches its maximum threshold and then remains constant.

3.3. Implementation using Finite element

In this section, we consider a rectangular domain. The solution of equation (1) together with the boundary conditions is obtained with the aid of the FreeFem++ software [9]. We compute the approximate solution by a finite element method of Lagrange type P1 for the spatial discretization. An Euler method is used for the time discretization. The interest of this method is the possibility of considering unstructured geometries [11]. We then trace the contour values of the density for different cases.

3.3.1. Variational formulation

We approximate the solution of equation (1) by a finite element method of Lagrange type P1 in space and an Euler method for the time discretization.

$$\frac{\partial \rho}{\partial t} - v\Delta\rho + \nabla_x\rho = f$$

Let v be a test function. We multiply the above equation by v and integrating over the domain

$$\int_\Omega \frac{\partial \rho}{\partial t} v \, d\Omega - v\int_\Omega \Delta\rho.v \, d\Omega + \int_\Omega \nabla_x\rho.v \, d\Omega = \int_\Omega fv \, d\Omega$$

Integrating by parts and applying the boundary conditions yields

$$\int_\Omega \frac{\partial \rho}{\partial t} v + v\int_\Omega \Delta\rho.\Delta v + \int_\Omega \nabla_x\rho.v - v\int_{\Gamma_3} v\frac{\partial \rho}{\partial \vec{n}} ds = \int_\Omega fv$$

$$\int_\Omega \frac{\partial \rho}{\partial t} v + v\int_\Omega \Delta\rho.\Delta v + \int_\Omega \nabla_x\rho.v = \int_\Omega fv + v\int_{\Gamma_3} v\frac{\partial \rho}{\partial \vec{n}} ds$$

Applying Green's formula, we have

$$\frac{d}{dt}(\rho(t),v)_H - \int_{\Gamma_1} v\frac{\partial \rho}{\partial \vec{n}} ds - \int_{\Gamma_2} v\frac{\partial \rho}{\partial \vec{n}} ds - \int_{\Gamma_3} v\frac{\partial \rho}{\partial \vec{n}} ds + \int_\Omega \nabla\rho.\nabla v \, ds + \int_\Omega \nabla_x\rho.v \, d\Omega = \int_\Omega f(x,y,t)v \, dv$$

Applying the boundary conditions we see that

$$\int_{\Gamma_1} v\frac{\partial \rho}{\partial \vec{n}} ds = 0, \qquad \int_{\Gamma_2} v\frac{\partial \rho}{\partial \vec{n}} ds = 0, \qquad \int_{\Gamma_3} v\frac{\partial \rho}{\partial \vec{n}} ds = \int_{\Gamma_3} vg(x,y,t)ds$$

Hence we have

$$\frac{d}{dt}(\rho(t),v)_H + \int_\Omega \nabla\rho.\nabla v \, ds + \int_\Omega \nabla_x\rho.v \, d\Omega = \int_\Omega f(x,y,t)v \, dv + \int_{\Gamma_3} vg(x,y,t)ds$$

Hence the variational problem can be written as: Given $f \in L^2(\Omega)$, find the value of $\rho \in V$ such that

$$\frac{d}{dt}(\rho(t),v)_{L^2(\Omega)} + a(\rho,v) = L(v)_{L^2(\Omega)}, \forall \, v \in V, t \in (0,T)$$

$$\rho(0) = 0$$

Where

$$\frac{d}{dt}(\rho(t), v)_{L^2(\Omega)} = \int_\Omega \dot{f}(x, y, t)v \ dv + \int_{\Gamma_3} \dot{v}g(x, y, t)ds$$

$$a(\rho, v) = \int_\Omega \dot{\nabla\rho}.\nabla v \ d\Omega + \int_\Omega \dot{\frac{\partial\rho}{\partial x}}v \ d\Omega$$

$$L(v) = \int_\Omega \dot{f}v \ d\Omega + \int_\Omega \dot{g}v \ d\Omega$$

We want to find $\rho_n : [0, T] \to V_n$ such that

$$\frac{d}{dt}(\rho_n(t), v_n)_H + a(\rho_n(t), v_n) = \langle f_n(t), v_n\rangle$$

$$(\rho_n(0), v_n)_H = (0, v_n)_H = 0$$

Let $\varphi_i, i = 1,2, \cdots, n$ be a basis of V_n, we have

$$\rho_n(t)(x, y) = \sum_{j=1}^n \rho_j(t)\varphi_j(x, y)$$

$$v_n(t)(x, y) = \sum_{j=1}^n v_j(t)\varphi_j(x, y)$$

$$\frac{d}{dt}\left(\sum_{j=1}^n \rho_j(t)\varphi_j, \sum_{j=1}^n v_j(t)\varphi_j\right)_H + a\left(\sum_{j=1}^n \rho_j(t)\varphi_j, \sum_{j=1}^n v_j(t)\varphi_j\right) = \left(f(t), \sum_{j=1}^n v_j(t)\varphi_j\right)$$

$$\sum_{j=1}^n (\varphi_i, \varphi_j)n \ \rho_j' + \sum_{j=1}^n a(\varphi_i, \varphi_j)\rho_j = (f(t), \varphi_i)$$

Where the Mass and Stiffness matrix are respectively

$$\sum_{j=1}^n (\varphi_i, \varphi_j), \sum_{j=1}^n a(\varphi_i, \varphi_j)$$

We prove the existence and uniqueness of the solution of the (non symmetric) variational problem:

Find $\rho \in V$ such that

$$a(\rho, v) = f(v) \forall v \in V,$$

where V is a Hilbert space, $F \in V$ and $a(.,.)$ is a continuous, coercive bilinear form that is not necessarily symmetric. The Lax-Milgram Theorem guarantees both existence and uniqueness of the solution to the variational formulation [11].

Firstly, we see that the space $V = H^1(\Omega)$ is a Hilbert space. The mapping a is a bilinear, continuous, coercive form of V:

$$a(\rho, v) = v \int_\Omega \nabla\rho.\nabla v \ d\Omega + \frac{\partial\rho}{\partial x} v d\Omega$$

$$|a(\rho, v)| = \left| v \int_\Omega \nabla\rho.\nabla v \ d\Omega + \frac{\partial\rho}{\partial x} v d\Omega \right|$$

$$\leq k \left(\int_\Omega |\nabla\rho.\nabla v| \ d\Omega + \left|\frac{\partial\rho}{\partial x} \cdot v\right| d\Omega \right) \ by \ triangular \ inequlity$$

$$\leq k \left(\int_\Omega \|\nabla\rho\|.\|\nabla v\| \ d\Omega + \left\|\frac{\partial\rho}{\partial x}\right\| \|v\| d\Omega \right) \ by \ schwartz \ inequality$$

$$\leq k \left(\|\nabla\rho\|_{L^2(\Omega)}.\|\nabla v\|_{L^2(\Omega)} + \left\|\frac{\partial\rho}{\partial x}\right\|_{L^2(\Omega)} \|v\|_{L^2(\Omega)} \right)$$

$$\leq k \left(\|\rho\|_{H^1(\Omega)}.\|v\|_{H^1(\Omega)} + \|\rho\|_{H^1(\Omega)} \|v\|_{H^1(\Omega)} \right)$$

$$\leq k \left(\|\rho\|_{H^1(\Omega)}.\|v\|_{H^1(\Omega)} \right)$$

Thus, a is continuous. We will now show that it is coercive.

The coercivity of the variational form in equation 24 can be proved in part by the Gårding inequality. By the Gårding inequality, there is a constant $K < \infty$

$$a(v, v) + k\|v\|^2_{L^2(\Omega)} \geq \frac{\alpha}{2} \|v\|^2_{H^1(\Omega)} \forall v \in H^1(\Omega)$$

Where α is a constant.

Thus, $a(v, v)$ itself may not be coercive, but adding a sufficiently large constant multiplied by the L^2-inner product makes it coercive over all $H^1(\Omega)$. We show this in the sequel.

$$a(v, v) + k\|v\|^2_{L^2(\Omega)} \geq \alpha\|v\|^2_{H^1(\Omega)} + \int_\Omega \frac{\partial v}{\partial x} v + kv^2 d\Omega$$

By Holder's inequality, we have

$$\int_\Omega \frac{\partial v}{\partial x} v \, d\Omega \leq \int_\Omega \left|\frac{\partial v}{\partial x}\right| |v| \, d\Omega$$

$$\leq \left\|\frac{\partial \rho}{\partial x}\right\|_{L^2(\Omega)} \|v\|_{L^2(\Omega)}$$

$$\leq C\|v\|_{H^1(\Omega)} \|v\|_{L^2(\Omega)}$$

Showing that $C\|v\|_{H^1(\Omega)} \|v\|_{L^2(\Omega)}$ is positive.

Hence, we get

$$a(v,v) + k\|v\|_{L^2(\Omega)}^2 \geq \alpha\|v\|_{H^1(\Omega)}^2 - C\|v\|_{H^1(\Omega)}\|v\|_{L^2(\Omega)} + \int_\Omega kv^2 \, d\Omega \geq \alpha\|v\|_{H^1(\Omega)}^2 - C\|v\|_{H^1(\Omega)} + k\|v\|_{L^2(\Omega)}$$

So that

$$a(v,v) + k\|v\|_{L^2(\Omega)}^2 \geq \frac{\alpha}{2}\|v\|_{H^1(\Omega)}^2 + \|v\|_{L^2(\Omega)}$$

Provided $k = \frac{\alpha}{2} + \frac{C}{2\alpha}$

$L(v)$ is continuous linear functional in V.

$$|L(v)| = \left|\int_\Omega fv \, d\Omega + \int_{\Gamma_3} gv \, d\Omega\right|$$

$$\leq \int_\Omega |f||v| \, d\Omega + \int_{\Gamma_3} |g||v| \, d\Omega$$

$$\leq \int_\Omega |f||v| \, d\Omega + \int_\Omega |g||v| \, d\Omega$$

$$\leq \|f\|_{L^2(\Omega)} \|v\|_{L^2(\Omega)} + \|g\|_{L^2(\Omega)} \|v\|_{L^2(\Omega)}$$

$$\leq \left(\|f\|_{L^2(\Omega)} + \|g\|_{L^2(\Omega)}\right) \|v\|_{L^2(\Omega)}$$

$$= \beta\|v\|_{H^1(\Omega)}^2$$

Thus a is also coercive. Hence by the Lax-Milgram theorem, we have the existence and uniqueness of the solution.
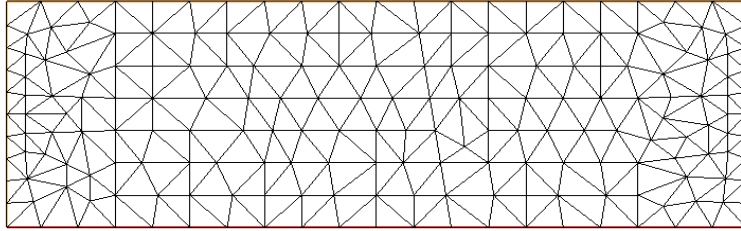
3.1.2 Implementation of FEM in FreeFem++

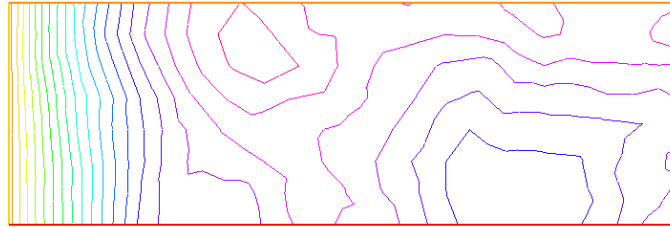Figure 7: Finite element mesh for the pollutant problem

Figure 8: Contour for the pollutant problem; f = 3, g = 0.5
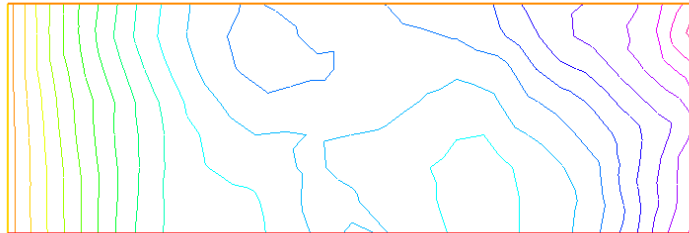

Figure 9: Contour for the pollutant problem; f = 3, g = 1.0

Figure 10: Contour for the pollutant problem; f = 10, g = 1.0

4. Discussion

In the case of the finite difference method, three schemes were employed to simulate the solution of the pollutant dispersion numerically. The Crank Nicolson scheme produced a much better results compared to the implicit and explicit Euler schemes. The results revealed that in the absence of divergence term, a high pollutant concentration was noticed within the canal. The inclusion of the divergence term led to the dispersion of pollutants in the direction of fluid flow.

Moreover, the behaviour observed in the finite element implementation is quite like that of finite-difference. Different plots were obtained for the different values of the source term f and the flux g across the boundary. It is observed that there is more concentration of the pollutant inside the canal when the flux across the boundary Γ_3 is small. The concentration becomes relatively well spread as the flux increases.

5. Conclusion

The proposed finite difference schemes for spatial discretization and the theta scheme for time converged as long as the given condition is satisfied. In contrast, implicit schemes converge unconditionally, allowing the use of large or minimal time/spatial steps. The model can be upgraded to 3D to simulate the flow of the pollutant down the stream. The result can be helpful in understanding situations where the water flows into another dam, river or the ocean, in which the amount of pollutant can affect aquatic life. Also, the model can be extended to include terms that account for the effects of life inside the canal. A limitation to the method is that it is still to be validated by experimental results within the same parametric study.

References

[1] Safia, M., Abdelkader, S., Mohamed, H., and Omar, H. (2015). Pollutant dispersion in natural streams using the transmission line matrix method. Journal of Interdisciplinary Mathematics, 20:317–330.

[2] Pawarisa, S., and Nopparat, P. (2018). Numerical simulation of a one-dimensional water quality model in a stream using a Saulyer technique with quadratic interpolated initial boundary conditions. Journal of Abstract and Analysis, 17:98–107.

[3] Launay, M., Le Coz, J., Camenen, B., Walter, C., Angot, H., Dramais, G., Faure, B., and Coquery, M. (2015). Calibrating pollutant dispersion in 1-D hydraulic models of river networks. Journal of Hydro-environment Research, 9:120–132.

[4] Wayjang, M., and Nopparat, P. (2015). A Numerical treatment of a one-dimensional form of a water-quality model in the Rama-nine reservoir. initial-boundary conditions. Journal of Interdisciplinary Mathematics, 18:375–394.

[5] Witsarat, K., and Nopparat, P. (2015). Implicit finite difference simulation of water pollution control in a connected reservior system. International Journal of Applied Mathematics, 45:98– 107.

[6] Kulmart, K., and Pochai, N. (2020). Numerical simulation for salinity intrusion measurement models using the MacCormack finite difference method with lagrange interpolation. Journal of Interdisciplinary Mathematics. 1-30

[7] Issakhov, A., Alimbek, A., and Zhandaulet, Y. (2021). The assessment of water pollution by chemical reaction products from the activities of industrial facilities: Numerical study. Journal of Cleaner Production. 282: 125239

[8] Pan, Y., Guo, J., Yang, L., Yuan, Q., Ren, Z., Wang, L. (2021). Numerical simulations of non-point source pollution in a small urban catchment: Identification of pollution risk areas and effectiveness of source-control measures. Water. 13, 96

[9] Hecht, F. New development in FreeFem++. Journal of numerical mathematics. 20 (2012), no. 3-4, 251-256. 65Y15

[10] Won, Y. Y., Wenwu C., Tae-Sang C., and John M. (2005). Applied numerical methods using MATLAB. John Wiley and Sons, Inc., Hoboken, New Jersey

[11] Susanne, C. B., and Scott L. R. (2008). The mathematical theory of finite element methods, third edition. Springer-Verlag, New York